The Analysis of Typhoon Structures Using Advanced Microwave Sounding Unit Data and Its Application to Prediction

CHIEN-BEN CHOU

Central Weather Bureau, Taipei, and Department of Atmospheric Sciences, National Central University, Jhong-Li, Taiwan

CHING-YUANG HUANG

Department of Atmospheric Sciences, National Central University, Jhong-Li, Taiwan

HUEI-PING HUANG

Lamont-Doherty Earth Observatory of Columbia University, Palisades, New York

KUNG-HWA WANG AND TIEN-CHIANG YEH

Central Weather Bureau, Taipei, Taiwan

(Manuscript received 6 September 2006, in final form 20 August 2007)

ABSTRACT

In this study, the Advanced Microwave Sounding Unit (AMSU) data are used to retrieve the temperature and velocity fields of typhoons and assimilate them with the three-dimensional variational data assimilation (3DVAR) routines for uses in numerical model predictions for typhoons. The authors' procedure of an end-to-end typhoon prediction using an AMSU-based initial condition is similar to the framework developed by Zhu et al. in 2002 but differs from it by considering a downward integration approach in part of the retrieval process and with the starting point of the integration chosen as a constant 50-hPa field without any structure. The typhoon circulation from this retrieval is thus determined objectively from the AMSU observation alone, without a preimposed typhoon vortex structure, allowing an asymmetric structure even at the inner core of a typhoon. The results show that this procedure is capable of retrieving a reasonable typhoon circulation from the AMSU data. The impact of the AMSU data on the assimilated initial condition for prediction is shown to be especially notable in its modification of the upper-level circulation of the typhoons. With the downward integration, the error accumulates downward such that the current approach provides a relatively more accurate estimate of the upper-level circulation, important for the steering of a typhoon. Consistent with this, it is demonstrated that the inclusion of the AMSU data helps to improve the forecast of typhoon tracks for selected cases of typhoons. This approach is less satisfying in producing an accurate retrieval and prediction of the intensity of typhoons. The reasons for this shortcoming and possible future remedies are discussed.

1. Introduction

Satellite measurements provide one of the most important data sources for the analysis and prediction of typhoons, whose genesis and development occur over the ocean where traditional observations are sparse. These measurements along a swath of several hundreds of kilometers in width may be retrieved to enhance the analysis of the atmospheric state including the obscured cyclone. For example, among many others, Chen et al. (2004) have attempted to assimilate Special Sensor Microwave Imager (SSM/I) microwave observations that enhance the delineation of the hurricane and thus improve the model prediction.

The Advanced Microwave Sounding Unit (AMSU) measurements are particularly useful for determining the structures of typhoons or hurricanes because of its high spatial resolution, in addition to the fact that microwave observations are not subject to the obstruction

Corresponding author address: Prof. Ching-Yuang Huang, Department of Atmospheric Sciences, National Central University, Jhong-Li 32045, Taiwan.
E-mail: hcy@atm.ncu.edu.tw

DOI: 10.1175/2007JAMC1577.1

of clouds. Early studies on the retrieval of the temperature, wind, and pressure structures of typhoons or hurricanes using microwave observations (Rosenkranz et al. 1978; Kidder et al. 1978, 1980; Grody et al. 1982; Velden et al. 1991) have paved the way for the development of a comprehensive AMSU-retrieval procedure for storm structures that can potentially be used for improving model predictions. This has been an important direction in typhoon research. For example, recently Kidder et al. (2000) and Knaff et al. (2004) have used AMSU data to derive the axisymmetric tangential wind of typhoon circulation as a function of radius and height from the retrieved temperature field, and then use it to study the relationship between the structures of a tropical cyclone and its environmental vertical shear.

For the application of AMSU data in typhoon/hurricane prediction that is of our major interest, Zhu et al. (2002, hereinafter Z02) have recently developed a comprehensive framework to retrieve the three-dimensional structures of Hurricane Bonnie (1998) from the AMSU data and to incorporate the retrieved vortex structure into a numerical weather prediction model. They showed promising results in the forecast that incorporated the AMSU data. Z02, which inspired this study, considered an upward integration of the retrieved temperature in order to obtain the geopotential height and then the velocity field of the hurricane circulation. The lower boundary condition for their upward integration is a surface pressure field with a prescribed circular inner core structure of the hurricane vortex, which is then gradually merged with the environmental pressure field (which can be asymmetric) far away from the center of the hurricane. The core structure of their hurricane is constrained by this prescription and is not objectively determined by the AMSU data alone. The upward integration also means that the error accumulates upward, likely leading to more accurate estimates of the low-level but less accurate estimates of the upper-level circulations, the latter being important for the steering of a typhoon or hurricane. Thus, within the already useful framework of Z02 there remain potentially interesting alternatives to explore.

Our study here aims to investigate one of such alternatives, by considering the approach in which the entire temperature and velocity structure of a typhoon is objectively determined by the AMSU observations, and then examining how the retrieved field thus produced can impact typhoon prediction when it is assimilated into the initial condition of a forecast model. A distinction between ours and the original procedure of Zhu et al. is that we integrate the retrieved temperature field downward from a constant 50-hPa field, thus removing any prescribed a priori constraint on the structure of the typhoon and, at the same time, emphasizing an accurate estimate for the upper-level circulations.

For the first part of our task related to retrieval, it is worth noting that a recent work by Bessho et al. (2006) has made similar advances in the technique. They adopted a two-step approach in the previously mentioned vertical integration, first integrating the temperature field upward, then smoothing the 50 hPa field, and then performing a downward integration. Thus, our approach for retrieval is in the same spirit as Bessho et al. (2006; we developed the strategy of downward integration independently, as previously reported in Chou et al. 2005). Nevertheless, our goal here is not just to perform the retrieval, but to use its product, that is, the derived 3D balance typhoon vortex, based on the framework of Z02, to conduct end-to-end predictions for typhoons. Direct assimilation of the AMSU-retrieved temperature for improving the analyses of typhoons also shows noticeable benefits for track prediction (Liang et al. 2007).

We will proceed with a description of the satellite data and the retrieval procedure in section 2, the detail of the forecast model and data assimilation system in section 3, results of retrieval and model predictions in section 4, and concluding remarks in section 5.

2. Satellite data and retrieval procedure

The retrieval of the structure of the typhoon circulation from the AMSU data takes several steps. The three-dimensional temperature field is first retrieved from the satellite observation. A vertical integration of the retrieved temperature leads to the height field, which is then used in a nonlinear balance equation to derive the velocity field. The following are further details of these steps.

a. Retrieval of temperature

Following Z02, we first retrieve temperature from the AMSU data by a statistical method. The retrieved temperature can be expressed as

$$T(p) = C_o(p, \theta_s) + \sum_{i=1}^{n} C_i(p, \theta_s) T_b(\nu_i, \theta_s), \qquad (1)$$

where $T(p)$ is the retrieved atmospheric temperature at pressure p and $T_b(\nu_i, \theta_s)$ is the brightness temperature from the AMSU-A measurement at channel frequency ν_i with scan angle θ_s. The coefficients $C_o(p, \theta_s)$ and $C_i(p, \theta_s)$ were established by matching the rawinsonde

temperature soundings with the AMSU-A brightness temperature for each scan angle (Z02). For the satellite observation, we use that produced by the *NOAA-16* satellite. The data were preprocessed daily at the Central Weather Bureau (CWB) of Taiwan using the Advanced Very High Resolution Radiometer (AVHRR) and Advanced Television and Infrared Observation Satellite (TIROS) Operational Vertical Sounder (ATOVS) Processing Package (AAPP). We used the level-1d data.

The statistical analysis in Eq. (1) produces the temperature at constant pressure levels. Since the procedure itself does not "know" where the surface is, it provides the temperature field even for the pressure levels below the surface. (This occurred only occasionally, since most of the typhoons are located over the ocean at the initial times in our forecast experiment.) Because the result of retrieval is not our final product but it only serves as the initial condition for the forecast, we choose not to modify the retrieval procedure to specifically accommodate orography at this stage, but leaving the treatment of topography to the next stage during data assimilation [three-dimensional variational data assimilation (3DVAR); see section 3].

The AMSU data used in this work were collected from June to July 2004 for the area in the vicinity of Taiwan. We have selected the observations in which a typhoon is fully covered by one swath. Note that although the more recent AMSU measurements are known to have problems with a high level of noise, they occurred after January 2005 and did not affect the June–July 2004 data used in this study (T. Mo 2007, personal communication). The AMSU channels 6–11 are used for the retrieval of temperature. Channels 1 and 2 are also used to estimate cloud liquid water and precipitation rate that will be useful later for deriving the divergent component of velocity (see section 2d). Channels 3, 4, and 5 are excluded from our procedure for temperature retrieval, because they are sensitive to the scattering by heavy rain and ice particles.

Recently, Bessho et al. (2006) and Demuth et al. 2004 have attempted to correct the bias in the AMSU-based retrieved temperature due to scattering by heavy rain and ice particles. We have not adopted this technique, but our exclusion of channels 3–5 at least alleviated the problem. For the AMSU channels we used, channel 6 may still be somewhat affected by scattering. This might contribute to occasionally large temperature anomalies in some cases. As will be discussed later, since we will adopt a downward integration approach to obtain the height and velocity fields from temperature, the derived upper-level circulation (above where heavy rain is occurring) will be less affected by this problem. Certainly, assessing the effect of scattering by large particles remains an important direction for future work. (An accurate assessment of this effect will eventually require in situ measurements of the microphysical properties of the rain/ice particles and detailed radiative transfer calculations for the microwave bands. These are beyond the scope of this paper.)

The coefficients in the algorithm in Eq. (1) were statistically established for each individual scan angle. As such, limb correction is not necessary for the radiance data. However, some slight kinks exist at the boundary between two scan angles which, if left untreated, can affect the retrieved temperature by creating an artificial temperature gradient, which could subsequently affect the height and velocity fields. Fortunately, the bias that arises from this problem is systematic and is removable by applying a filter along the scan line. More detail on this point will be explained in section 2e using an example of a retrieved flow field.

b. Derivation of the height field

With the retrieved temperature, the three-dimensional geopotential height field can be obtained by a vertical integration of temperature assuming hydrostatic balance. As mentioned in the introduction, Z02 considered an upward integration of the temperature from a given surface pressure field with an imposed circular inner core structure of the typhoon vortex, which is matched with the environmental (and generally asymmetric) pressure field far away from the storm center. While this approach has its advantage (e.g., it guarantees a clear vortex structure at the core of a typhoon), the imposed vortex structure is artificial and may depart from the true structure of a particular typhoon. With the upward integration the constraint imposed at the surface will affect the flow structure at all levels. To explore an alternative, we instead adopt the assumption of Kidder et al. (2000) that the geopotential height at the 50-hPa level is uniform, and then integrate the retrieved temperature downward to obtain geopotential height. Specifically, the 50-hPa height for the area containing a typhoon is evaluated from the environmental data (outside the typhoon) for which the surface pressure is provided by a numerical weather prediction system (see section 3). (The surface pressure and temperature outside the typhoon are clearly defined and can be used to determine the height at 50 hPa by the hydrostatic equation.) Because there is no imposed a priori structure at 50 hPa, in our approach the structure of the height and velocity fields will be determined entirely by the AMSU observation through the retrieved temperature.

There are pros and cons for the two approaches with a downward and upward integration. With the downward integration, the error accumulates downward such that we may have more accurate estimates of the upper-level circulation but less accurate estimates of the low-level circulation. The opposite is true for the upward integration. Also, the structure of the flow field of a typhoon is usually more complicated at the surface than at 50 hPa (in fact, the structure of a typhoon is to about vanish at that level). If the uncertainty in the flow or pressure field (based on other non-AMSU observations) at the surface is greater than that at 50 hPa, it might be beneficial to consider a downward integration. As mentioned in section 1, recently Bessho et al. (2006) have considered a two-step approach by first doing an upward integration followed by smoothing of the resulted 50-hPa field, and then taking a downward integration. Our procedure is simpler, only considering a downward integration from a constant 50-hPa field.

c. Derivation of the rotational component of velocity

After the three-dimensional height field is derived from the retrieved temperature, we then solve a nonlinear balance equation at each pressure level to obtain the streamfunction (or the rotational component of the velocity). The nonlinear balance equation is

$$\frac{1}{2}(\psi_{xx}+\psi_{yy}+f)^2-\frac{1}{2}(\psi_{xx}-\psi_{yy})^2-2\psi^2_{xy}+(\psi_x f_x+\psi_y f_y)-\left(\Phi_{xx}+\Phi_{yy}+\frac{1}{2}f^2\right)=0, \quad (2)$$

where ψ is the streamfunction, Φ is the geopotential height, and f is the Coriolis parameter. Our procedure of solving Eq. (2) is similar to Z02, detailed in their section 3b. An iterative (relaxation) method is used. When the ellipticity condition (see Z02) is violated at a location, Zhu et al. reset the negative value of the "Z" term [the last term of Eq. (2)] to zero. We used a similar strategy but reset the value of streamfunction at a grid point to the average of its neighboring points when the ellipticity condition is violated. While this is a compromise, the outcome of this procedure remains effective and useful because there are only a small number of grid points (e.g., Zhu et al. reported less than 5% of the grid points) that encounter the violation of the ellipticity condition. As also noted by Zhu et al., in the cyclonic region (where the major typhoon circulation is located) the ellipticity condition is seldom violated.

d. Divergent component of velocity

The solution of the balance equation only gives the rotational component of the velocity. Similar to Z02, the divergent component of the velocity is calculated following Tarbell et al. (1981), that is, by solving the omega and continuity equations. In the omega equation, the vertical distribution of latent heat is related to the precipitation rate, which can be estimated from the AMSU data (channels 1 and 2; see section 2a) as described by Grody et al. (2000). The surface stress that is needed as the lower boundary condition is estimated from a bulk aerodynamic formula (Smith 2003).

From the procedures in sections 2a–2d we obtain the 3D temperature and velocity fields of the typhoon that can be used for improvement of the initial analysis for forecast.

e. Examples and further detail on bias correction

Last, we continue from the end of section 2a to finish the discussion on the bias correction. Recall that because the coefficients in Eq. (1) were established for the individual scan angles, a slight kink can appear in the retrieved temperature field at the boundary of two scan angles. This bias is systematic and can be corrected with a filtering of temperature along the scan line. Figures 1 and 3 show examples of the retrieved temperature and wind field at 950 hPa before (Fig. 1) and after (Fig. 3) the bias correction. The unfiltered field in Fig. 1 has an unexpected northward flow, along the direction perpendicular to a scan line, that appears to the southeast of the main typhoon circulation. (See the flow near the bottom and to the left of the 130°E longitude.) The structure of the bias embedded in Fig. 1 can be extracted from the statistics of retrieved temperature anomalies obtained from quiescent regions where there are no weather disturbances, as illustrated in Fig. 2. In this figure, the temperature anomalies (which in the quiescent regions mainly reflect the biases) at different vertical levels are shown as a function of the scan position. (The center of the figure is the nadir.) The fact that the temperature anomalies are almost symmetric with respect to the nadir (note that the right half of Fig. 2 resembles the mirror image of the left half of it) confirms that the biases are related to the kinks between the scan angles and that they are systematic. The information in Fig. 2 is used to filter out the bias. After the bias correction, Fig. 3 shows that the unusual feature of the northward flow in Fig. 1 is reduced. It is also worth noting that, from Fig. 2, the problem with the kinks is more notable only away from the nadir. If a typhoon is located close to the nadir, the bias is minor to begin with.

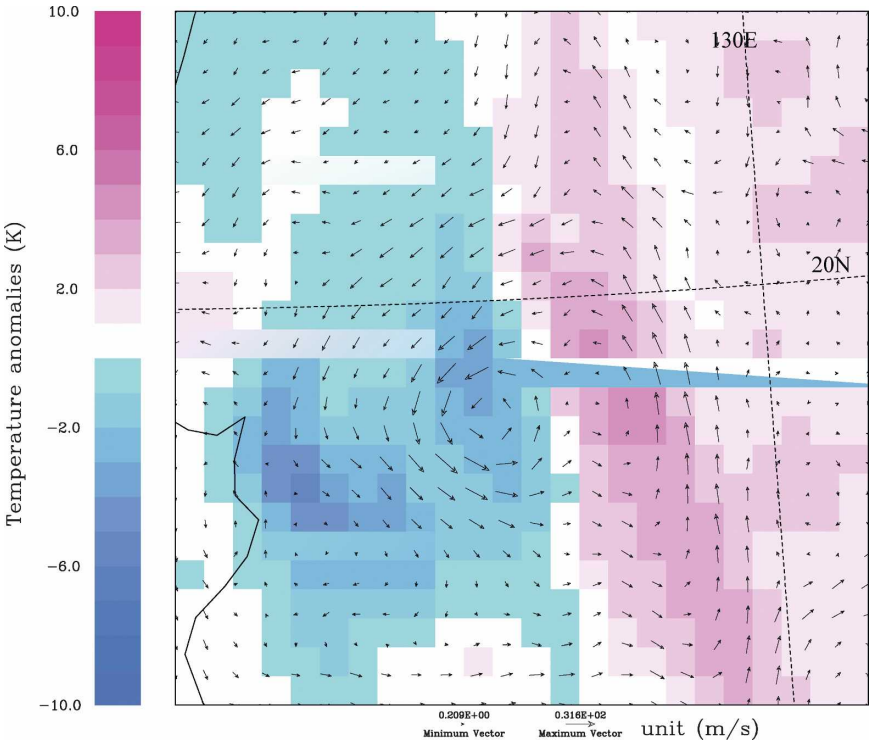

FIG. 1. The horizontal wind field (vectors) and the temperature field (image; shown is the anomaly defined as the departure from the value averaged over the domain boundary) at 950 hPa derived from the AMSU data at 0553 UTC 28 Jun 2004 for Typhoon Mindulle. The typhoon is located at the edge of scan. The color scale for temperature anomaly is indicated at left.

3. Data assimilation and the forecast system

To assess the impact of the AMSU data on typhoon prediction, we next assimilate the retrieved typhoon fields with a 3DVAR package, and then use the resulting initial condition to forecast with a regional numerical prediction model. The numerical prediction model we used is the nonhydrostatic fifth-generation Pennsylvania State University–National Center for Atmospheric Research Mesoscale Model (MM5; Dudhia 1993). The 3DVAR system that we used was developed for the MM5 model and was described in Barker et al. (2004, hereinafter B04).

The 3DVAR system generates an optimal estimate of the true atmospheric state at the analysis time by minimizing the cost function $\mathbf{J}(x)$ with respect to the atmospheric state x (e.g., Ide et al. 1997). Assuming that the probability distribution function of the observation and background error covariances is Gaussian with a zero mean, the cost function can be expressed as

$$\mathbf{J}(x) = (x - x^b)^{\mathrm{T}}\mathbf{B}^{-1}(x - x^b) + [y(x) - y^o]^{\mathrm{T}}(\mathbf{E} + \mathbf{F})^{-1}[y(x) - y^o], \quad (3)$$

where x^b is a background state with estimated error covariance matrix $\mathbf{B}$, y^o is observation, $y(x)$ is a forward operator that maps the model analysis x into the observation space, $\mathbf{E}$ is the expected error covariance matrix of the observation, and $\mathbf{F}$ represents error covariance matrix of the forward operator. The detailed procedure can be found in B04.

B04 have briefly tested the assimilation of a sea level pressure (SLP) at the typhoon center which was prescribed as observation. The 3DVAR system then adjusts the background field to generate a typhoon-like structure in the initial condition. (This is called the P-Bogus experiment by B04). Our situation here is different with certain advantage. We already have the comprehensive 3D structure of the typhoon field as retrieved from the AMSU data and may assimilate it directly with 3DVAR. This is more akin to the situation of having a very high density of sounding observations that cover the entire typhoon circulation. Also, note that, since our retrieval procedure does not objectively determine the absolute sea level pressure, our inputs to the 3DVAR system are the temperature and velocity fields on pressure levels as described before. We adopt

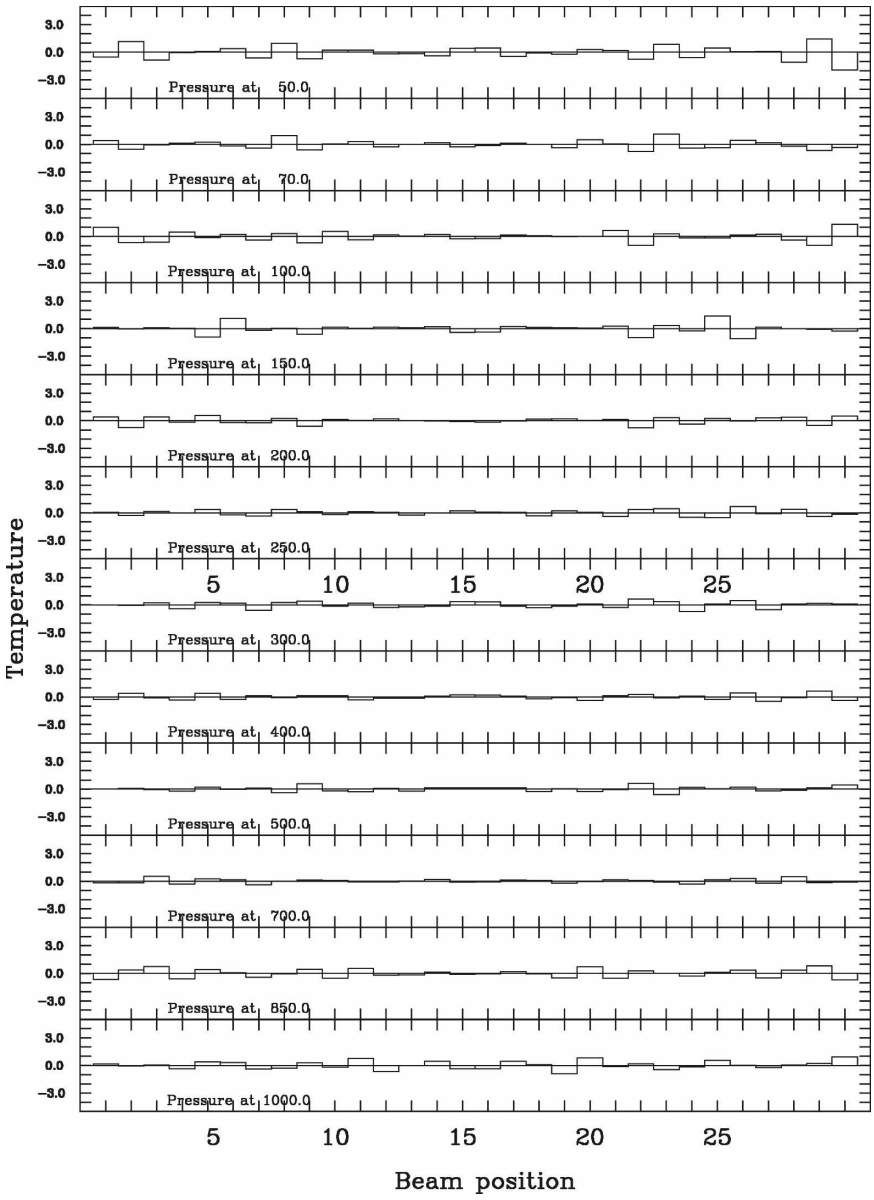

FIG. 2. The kinks between scan angles from the statistics of the retrievals for many observation paths. Shown are the retrieved temperature anomalies as a function of height and scan position obtained from a quiescent region.

the default setting in the 3DVAR system for the observation error; that is, the observation error is set to the "conventional" values for soundings. Then, the background error is subjectively adjusted such that the weight to the AMSU data is large enough for the AMSU input to have an impact on modifying the initial condition. In principle, this last step could be done more objectively, but this would be a complicated task that requires running a large number of 3DVAR and forecasts for many typhoons, then statistically inferring the best parameter values for the background/observation errors from the validation of the forecasts. This approach is not pursued here because of the very limited cases of typhoons we have.

Our inputs to the 3DVAR system are the retrieved temperature and velocity fields at pressure levels. Essentially, we let these two fields to adjust to other conventional variables to produce the final typhoon circulation in the initial condition. The intensity of the typhoon (e.g., in terms of the minimum SLP) is then primarily determined by the two AMSU-based input fields. No extra interference (e.g., a "bogus surface

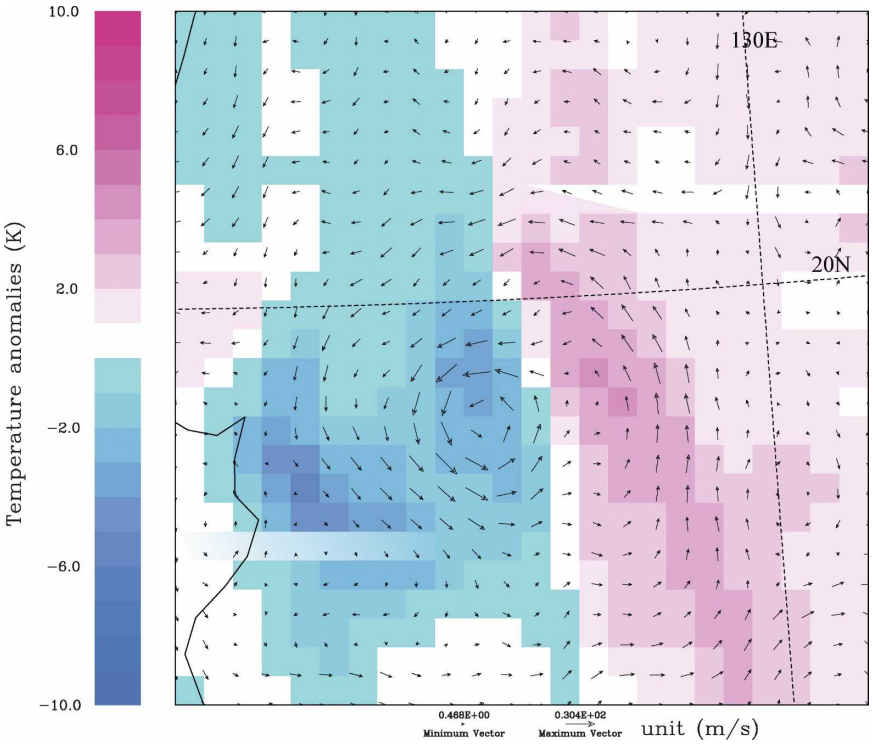

FIG. 3. As in Fig. 1, but with the kinks between scan angles smoothed.

pressure" approach of B04 by artificially adding a surface pressure perturbation at the center of a typhoon to enhance its minimum SLP) is performed. We found that this generally leads to an underestimate of the typhoon intensity. But we choose to leave it as is, given that our purpose is to assess how the assimilation of AMSU data alone impacts the forecast. Note that if an artificial perturbation is added to the SLP to be assimilated with the AMSU inputs (e.g., Liang et al. 2007), the former would smear or possibly disrupt the detailed structure of the typhoon circulation in the latter that we have painstakingly derived from the retrieval procedure. We leave the solution to this dilemma to future work. The issues with the typhoon intensity will be revisited in section 4c with more detail.

As noted in section 2a, we did not modify the retrieval scheme in Eq. (1) to specifically accommodate orography at the lower boundary. (Note, however, that in our forecast experiments to be conducted later the typhoons in the initial states are located mostly over the ocean.) Our retrieved temperature and velocity fields are at the pressure levels, possibly including those that are below the surface. Practically, we leave the treatment of topography to the data assimilation process (the 3DVAR package contains the full topography identical to the forecast model), through which the flow field is trimmed and adjusted to be consistent with the model topography.

In addition to the retrieved typhoon field, the other conventional fields that are needed to initialize and run the MM5 model for forecast are generated by a regional numerical weather prediction model; we use the operational NWP model of the Central Weather Bureau of Taiwan (Jeng et al. 1991; Liou et al. 1997). Once the initial condition is produced by 3DVAR, the MM5 model is used for the forecast. The MM5 model's horizontal resolutions are 45 km and 15 km in two nested grids. In the vertical, there are 24 levels.

4. Results

a. Analysis of the structures of typhoons

The first case to be analyzed is Typhoon Meari (2004) at 0457 UTC 29 September when it was on track toward Japan. Figures 4 and 5 show the retrieved temperature anomalies and horizontal wind fields at 850 and 250 hPa, respectively, using the procedure described in section 2a. Note that unlike in Z02, we did not impose an inner core structure of the typhoon in our procedure. The structures of the typhoon circulations in Figs. 4 and 5 are entirely objectively determined by the information in the AMSU observations.

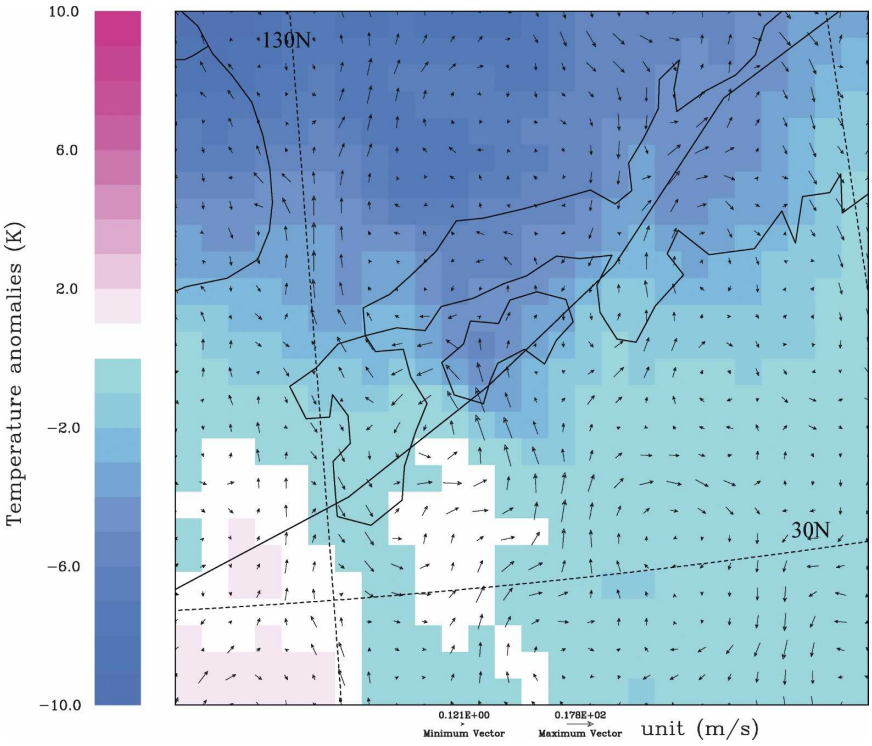

FIG. 4. The retrieved 850-hPa temperature anomaly (image) and horizontal wind field (vectors) derived from a balance equation for Typhoon Meari at 0457 UTC 29 Sep 2004. The solid line is the track of the typhoon that moves from southwest to northeast. The magnitude of the maximum vector is 17.8 m s^{-1} as indicated at the bottom.

Notably, the circulation center of the typhoon at 850 hPa does not coincide with that at 250 hPa (the center tilts slightly northeastward with height), likely because cold air coming from the north eroded the lower-level thermal structures of the typhoon. At the upper level (250 hPa) where the influence of the low-level inflow of cold air is not strong, the circulation center is closer to the maximum of the temperature anomaly. The circulation at 850 hPa shown in Fig. 4 is representative of those at other levels from 950 to 500 hPa (not shown). In general, the circulation of the typhoon is not axisymmetric. The southern branch of the vortex is stronger than the northern one at 250 hPa. At the lower levels, the northerly inflow of cold air tends to destroy the axisymmetric thermal structure of the typhoon. It might have also reduced the moving speed of the typhoon, given that the direction of the cold airstream is opposite to that of the track of the typhoon.

The next case is Typhoon Mindulle (2004) at the analysis time of 0541 UTC 29 June when it was developing over the tropical ocean in the vicinity of the Philippines and was slowly moving westward. Figure 6 shows that the retrieved temperature anomaly and horizontal wind field at 850 hPa for this typhoon are more axisymmetric than the first case shown in Fig. 4. Figure 7 shows a vertical cross section of the tangential wind field associated with this typhoon. The center of this typhoon is well defined at all levels below 100 hPa, and it does not significantly tilt with height. The intensity (measured by the magnitude of the maximum tangential velocity) of the typhoon also does not change significantly through the troposphere. These structures, derived from the AMSU data, indicate that the tropical cyclone has developed into the mature stage at this time. Comparing the vertical cross section in Fig. 7 to the analysis field produced by the Central Weather Bureau in Fig. 8, we find that the overall structures of the two wind fields are qualitatively similar but with some marked differences in detail. (The "analysis field" in Fig. 8 was constructed by first imposing an artificial Rankine vortex structure to mimic the velocity field of a typhoon, deriving the mass field from the velocity field of that vortex, and then merging them with conventional observations.) The radius of the typhoon, measured by the distance between its center and the location of the maximum wind, is smaller in the circulation derived from AMSU in Fig. 7. In the analysis field in Fig. 8 the tangential velocity decreases more

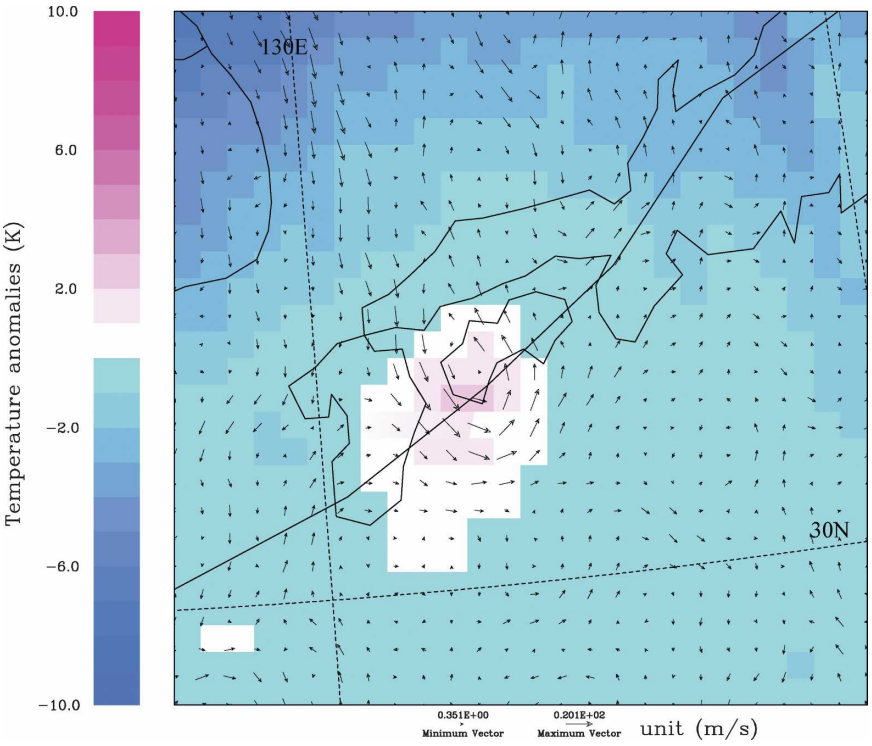

FIG. 5. As in Fig. 4, but for the 250-hPa level. The magnitude of the maximum vector is 20.1 m s^{-1}.

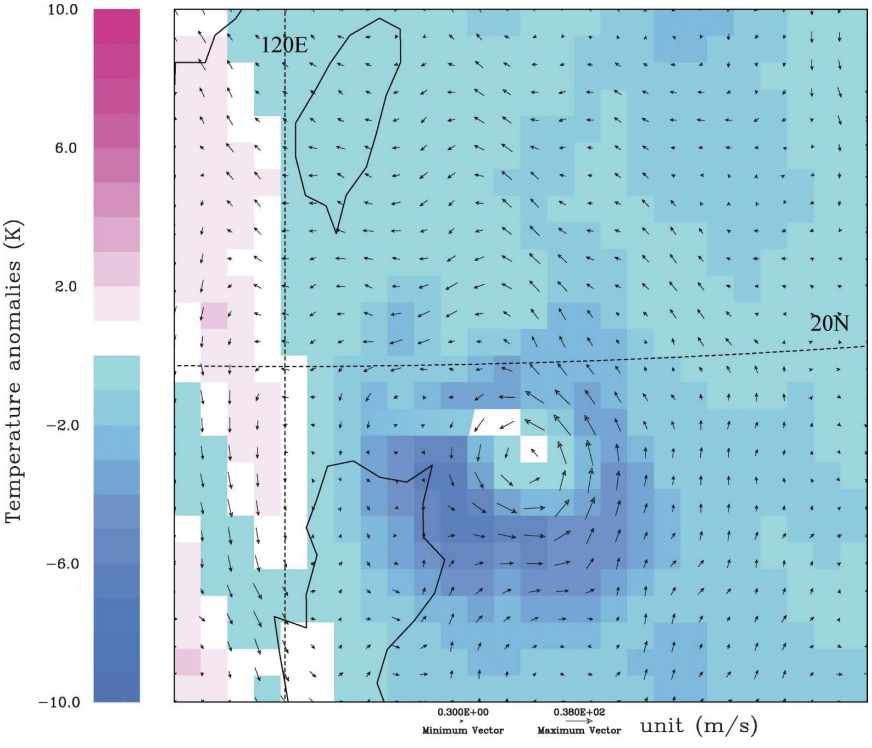

FIG. 6. As in Fig. 4, but for Typhoon Mindulle at 0541 UTC 29 Jun 2004. The typhoon is moving from east to west. The magnitude of the maximum vector is 38 m s^{-1}.

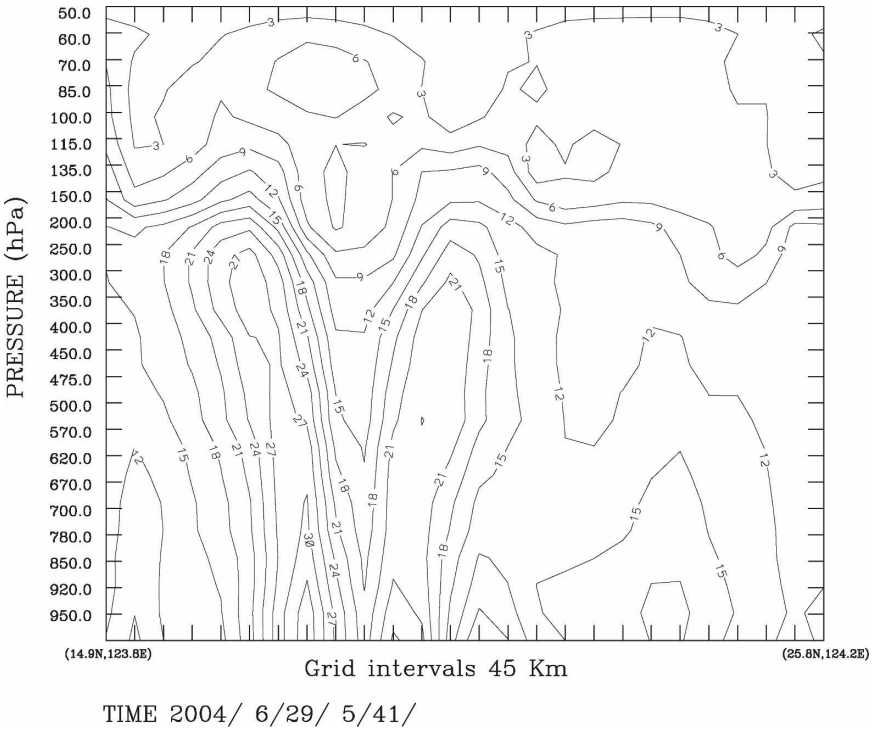

FIG. 7. A vertical cross section of the tangential wind derived from the AMSU data for the same typhoon and selected time as shown in Fig. 6.

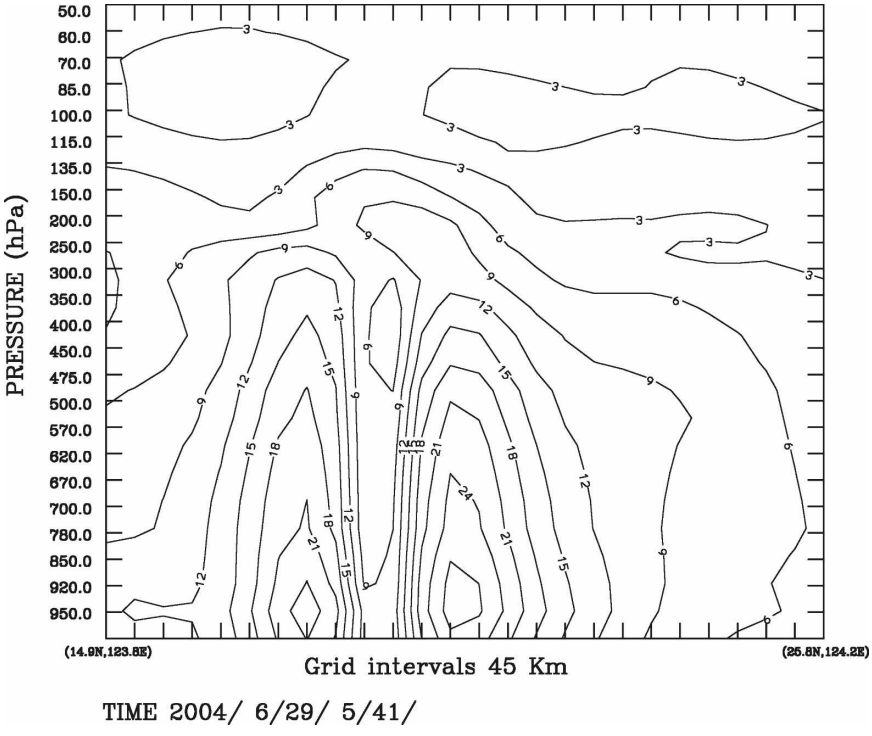

FIG. 8. As in Fig. 7, but for the analysis based on the operational regional model of CWB.

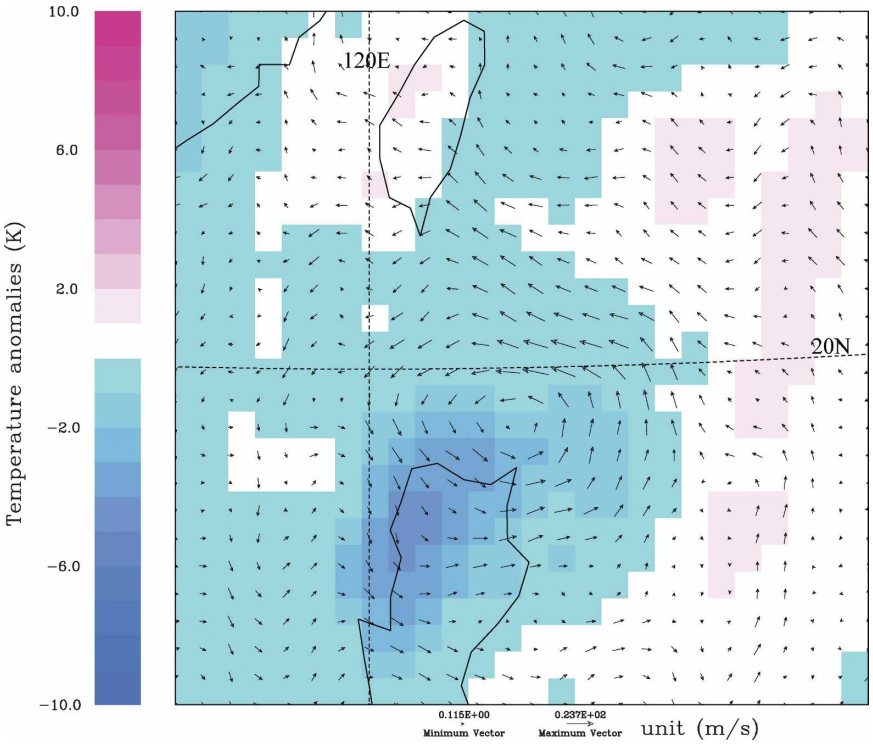

FIG. 9. The retrieved 500-hPa temperature anomaly (image) and horizontal wind field (vectors) at 1812 UTC 29 Jun for Typhoon Mindulle. The magnitude of the maximum vector is 23.7 m s^{-1}.

rapidly with height, such that at the upper troposphere the AMSU-derived wind is stronger than that in the analysis. This reflects one of the major impacts of the AMSU data, namely, the modification of the upper-level circulation. Also, recall that with the downward integration approach in our retrieval procedure, the error accumulates downward such that the retrieved upper-level circulation is generally more reliable.

Figure 9 shows the retrieved structures of the same typhoon at 500 hPa but for a later time at 1812 UTC 29 June. A closed circulation is still well defined for the typhoon, but its shape becomes more elliptical (this is true for most of the lower troposphere up to 400 hPa, not shown). The structures shown in Figs. 6–9 will again be referred to in our forecast experiments.

Although the elliptical shape of the retrieved typhoon circulation in Fig. 9 appears "unusual," an examination of the images of clouds from independent satellite (visible channel) observations reveals that the shape of the clouds associated with the typhoon at this time is indeed significantly elliptical (not shown). In contrast, the cloud images taken at the time corresponding to the case in Fig. 6 show a more circular shape for the typhoon (not shown), again agreeing with our retrieved circulation pattern for that case. Thus, both the circular structure in Fig. 6 and the elliptical pattern in Fig. 9 are likely real; the latter is not an artifact due to biases in the data.

b. *Forecast experiments*

The MM5 model along with its 3DVAR data assimilation system (B04), as described in section 3, are used for the forecast experiments. Our first forecast is for Typhoon Mindulle with an initial condition at 1800 UTC 29 June when the AMSU measurements covered the typhoon at 1812 UTC on the same day. Figure 10 shows the best-track analysis (circle) from Central Weather Bureau, the predicted track with the model initialized with the AMSU data (dot), and the predicted track in the "control" run without AMSU data (plus sign). The results indicate that the predicted track is closer to the observation (i.e., the best track) when the AMSU data are assimilated into the initial condition. Figure 11a shows the 500-hPa wind field and sea level pressure of the initial state (produced by 3DVAR) that incorporates the AMSU data. When compared with Fig. 9 (the retrieved wind field before it is assimilated with 3DVAR) the asymmetry (stronger wind in the northern branch of the vortex) in the typhoon circulation at 500

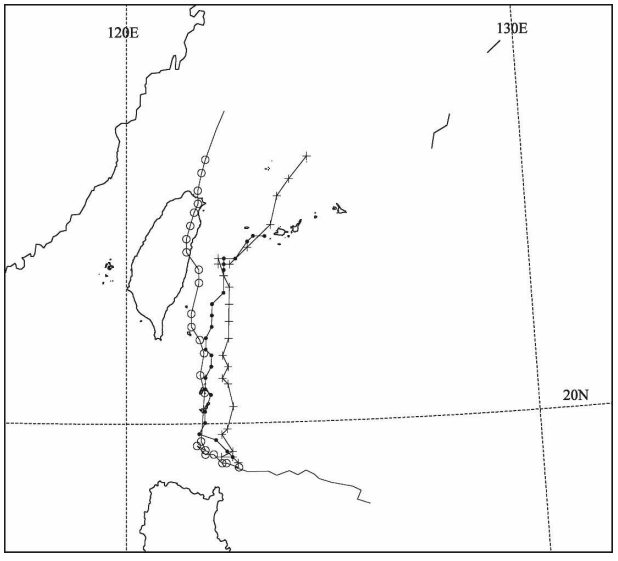

FIG. 10. The tracks of Typhoon Mindulle (2004). Shown are the best track (lined with circles) from CWB, the track (lined with crosses) for the control run, and the track (lined with dots) for the assimilation run that incorporates the AMSU data in the initial condition. The predictions are with 72 h of forecast time, with the interval between two consecutive symbols 3 h.

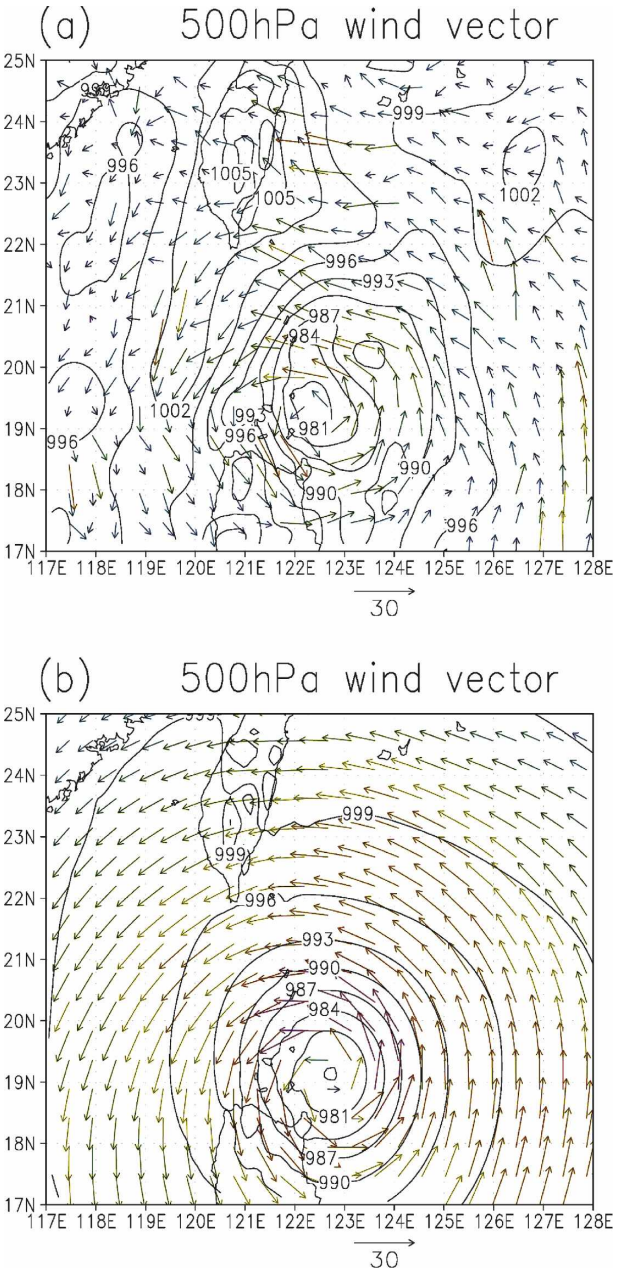

FIG. 11. The sea level pressure (contours) and 500-hPa wind field (vectors) of Typhoon Mindulle at 1812 UTC 29 Jun 2004. (a) The initial field that incorporates the AMSU data and (b) the initial field without the AMSU data. An arrow at the bottom of each panel indicates a wind vector with a magnitude of 30 m s^{-1}. To compare the magnitude of the wind vectors in the two panels, the vectors are colored according to their magnitude, from the weakest in blue to the strongest in red.

hPa is preserved in the initial condition for the model. Figure 11b shows the initial condition without incorporating the AMSU data. The vortex is more axisymmetric in both wind and pressure fields. The fact that the initial condition in Fig. 11a leads to a better forecast of the track indicates that the track of the typhoon is affected by the asymmetry of the vortex. For this case, it is also interesting to note that the impact of the AMSU data is more on the structure of the typhoon than on its intensity, as the minimum surface pressure remains about the same (980 hPa) in both Figs. 11a and 11b. As noted in section 3a, the surface pressure in these figures is generally not as low as that observed. We will discuss the issue with typhoon intensity in detail in section 4c. The observed Figs. 12a and 12b compare the initial wind fields in the west–east vertical cross section with and without the AMSU data, respectively. The asymmetry in the wind field is evident in the former with stronger wind shear. The incorporation of the AMSU data also renders the typhoon circulation above 450 hPa weaker than the case without the AMSU data. Otherwise, the maximum velocity at the lower troposphere is about the same for the two cases.

The next forecast is also performed for Typhoon Mindulle but with an earlier initial condition at 0060 UTC 29 June. The structure of the typhoon at that time as retrieved from the AMSU data was shown in Fig. 6. As mentioned before, this is a case when the typhoon circulation does not depart significantly from axisymmetry. As such, the initial conditions for the two runs with and without the input of AMSU data (not shown) are more similar to each other than the contrasting case shown in Figs. 11 and 12. Consequently, we expect the forecasts of the typhoon tracks for the two runs to

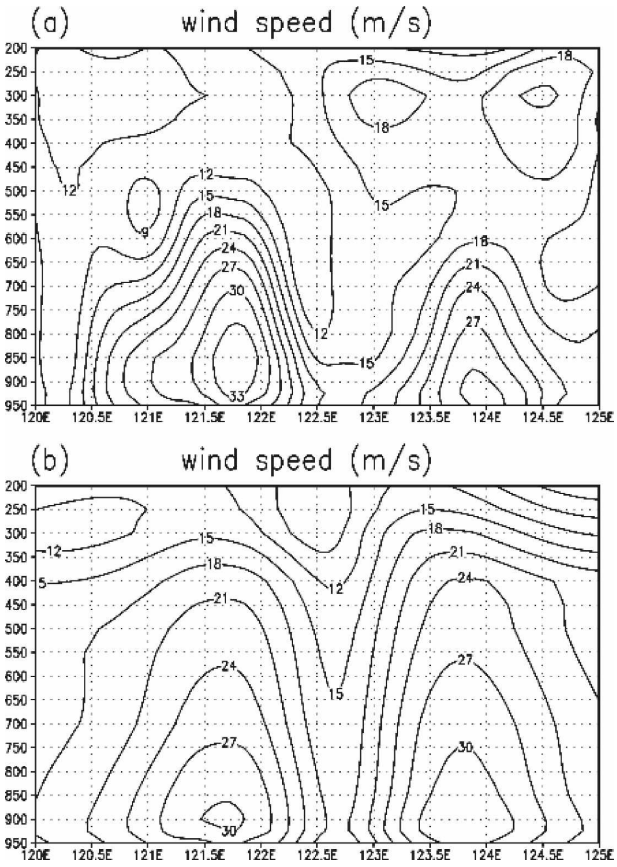

FIG. 12. The vertical east–west cross section of the tangential wind through the typhoon center at 1812 UTC 29 Jun 2004. (a) The initial field that incorporates the AMSU data and (b) the initial field without the AMSU data.

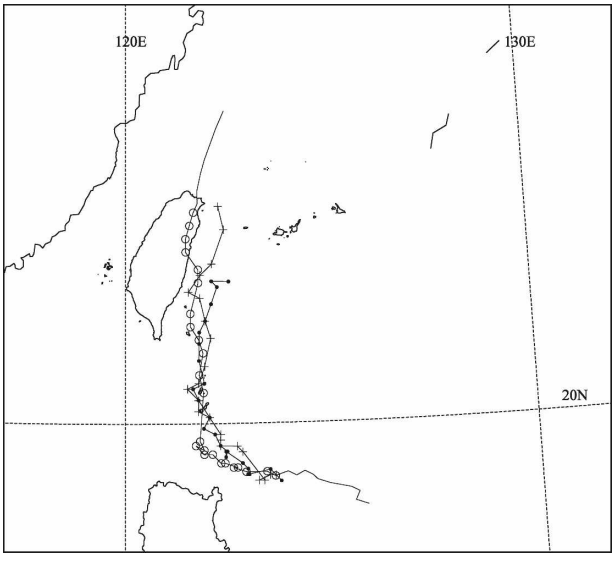

FIG. 13. As in Fig. 10, but for the experiments starting from the initial time of 0600 UTC 29 Jun 2004. The formats for the symbols are the same as in Fig. 10.

be more similar, which is indeed the case as shown in Fig. 13.

The last forecast is for Typhoon Mindulle starting from a later initial condition at 1800 UTC 30 June. This is only about 24 h before the landfalling of the typhoon in Taiwan. The initial states with and without the input of the AMSU data are shown in Fig. 14. Because the typhoon was close to the island at this time, the outflow of the vortex already interacted with the orography and the complicated lower boundary of the island surface. As a result, the inclusion of the AMSU data produces an irregularly shaped vortex in the initial state (Fig. 14a) while the analysis field without the AMSU data is more circular (Fig. 14b).

As the typhoon begins to interact with land, the predicted track is not as clearly defined as that over open ocean. In the following, we will instead show a sequence of the simulated circulations to compare the two runs. During the first 12 h of simulation, the typhoons for both runs move northward to approach Taiwan. The simulated 500-hPa wind and sea level pressure at 18, 24, and 36 h for the two runs are shown in Fig. 15. From 18 to 24 h, the typhoon for the run with the AMSU data moved closer to Taiwan than the control run without the AMSU data. In the former, the typhoon made landfall in Taiwan at around 24 h as observed. At this time, the simulated typhoon began to split when crossing the Central Mountain Range in Taiwan. A secondary sea level pressure minimum formed to the west of the mountain. After vigorous interactions with the island, the typhoon eventually left and moved northward by 36 h. In contrast, in the control run without the AMSU data, the core of the vortex remained to stay to the east of the island all the time (i.e., without landfall) and kept moving northward until eventually turning northeastward.

Overall, starting from an initial state incorporating the AMSU data, we have demonstrated a promising improvement in typhoon forecast. The assimilation of the AMSU data into the initial condition has a measurable and positive impact on the prediction of the track. Figure 16 summarizes the absolute errors in the forecast of the typhoon tracks averaged over the three cases in this study for the lead times from 0 to 72 h. In general, the forecast with the AMSU input performs better, especially within the range of 12–36 h. The results in this section also indicate that our modified approach—using a downward, instead of upward, integration to obtain the asymmetric height field and the circulation from temperature—is not only feasible but also proven to be beneficial, at least for the prediction of the tracks.

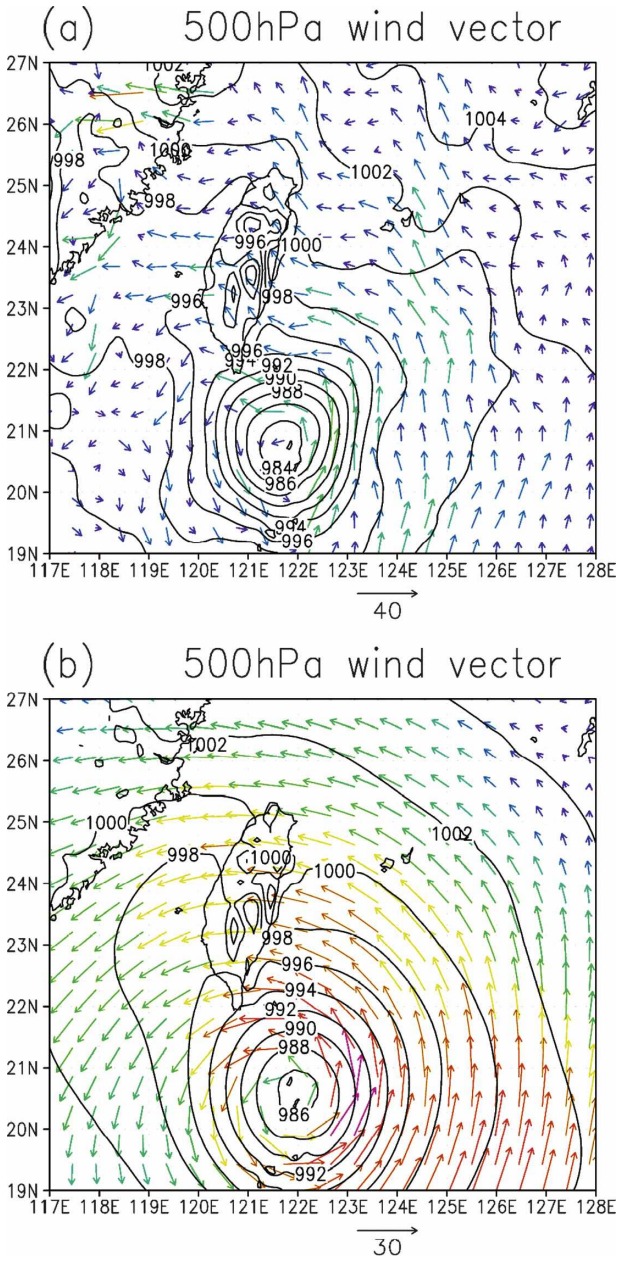

FIG. 14. As in Fig. 11, but for the experiments at the initial time of 1800 UTC 30 Jun 2004.

c. *Remarks on the forecast of typhoon intensity*

We have so far emphasized the uses of the AMSU data in the prediction of typhoon tracks. Within our framework, the retrieval and prediction of the intensity or SLP are more complicated, which we should now discuss. Figure 17 shows the time evolution of the minimum SLP from the observation (the best estimates from the Central Weather Bureau) and the pair of forecasts (with and without AMSU input) for the three cases studied in this work. It is evident from the figure that our forecasts underestimate the minimum pressure or the intensity of the typhoons from the very beginning. This is, in fact, not unexpected given the limitations in our approach as the following. First, recall that our retrieval procedure does not produce the absolute pressure field or SLP. The statistical procedure in Eq. (1) produces the temperature at pressure levels, $T(p)$, which was then used to derive the height and velocity fields, also on the pressure level. The AMSU data, which we have intended to use exclusively for constructing the initial typhoon field, do not provide precise information of the absolute value of the SLP. As such, only the retrieved temperature and wind at pressure levels are assimilated with 3DVAR in our experiments. (Note that the "SLP" field in Z02 was prescribed with extra assumptions and was not the result of an objective retrieval using the AMSU data.) The initial SLP field shown in the top panel of Figs. 11 and 14 is the product of 3DVAR after we assimilated the retrieved temperature–velocity fields with other conventional variables. In other words, the AMSU data affect the assimilated SLP only through the influences of the retrieved temperature/velocity fields for typhoon, when these fields are mutually adjusted with other conventional variables. But apparently, this alone is not enough to reproduce the reported minimum SLP (see Fig. 17). Thus, in this work the retrieval and prediction of typhoon intensity is less satisfying than that of typhoon tracks. The latter depends on the kinematic steering of a typhoon by the upper-level circulation that can be more usefully improved with the AMSU data.

Certainly, during the stage of performing 3DVAR we could artificially add an enhanced surface pressure depression at the center of the typhoon vortex (akin to the "P-Bogus" experiment in B04) to enhance the depression in SLP, but doing so would disrupt the structure of the typhoon circulation that was retrieved from the AMSU data, thereby somewhat negating our purpose of delineating the impact of the AMSU data alone on the forecast. A solution to this dilemma would be a useful direction for future work.

Another reason why the forecast of intensity is not improved by much with the AMSU data might be that the AMSU channels 6–11 do not provide additional information for moisture, which could also be important for the forecast for the intensity of typhoons (e.g., Chen et al. 2004).

5. Concluding remarks

In this work, the AMSU data are used to retrieve the temperature and velocity fields of typhoons and assimi-

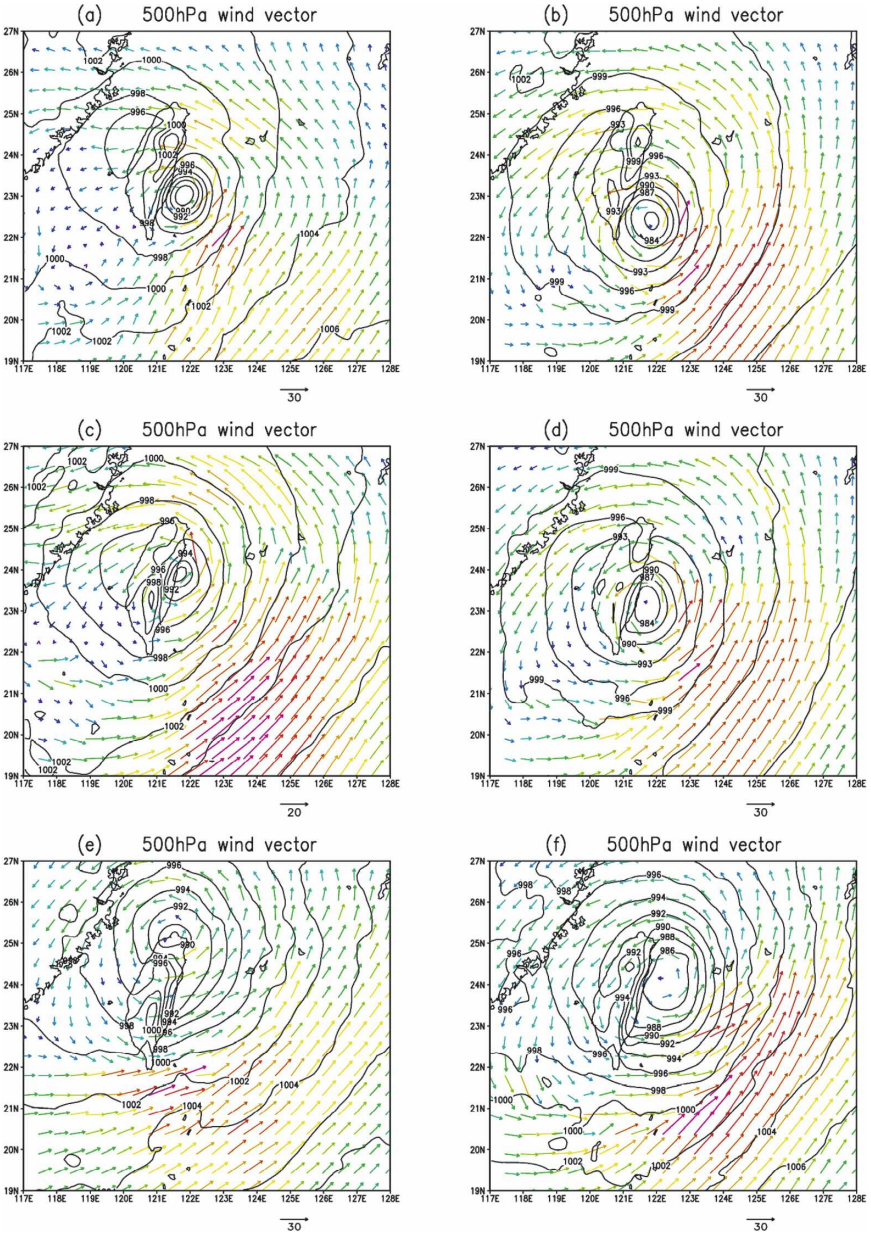

FIG. 15. As in Fig. 14, but for the simulated 500-hPa wind (vectors) and sea level pressure (contours) at (top) 18, (middle) 24, and (bottom) 36 h. Shown are the forecasts (left) with and (right) without assimilation of the AMSU data in the initial condition.

late them with the 3DVAR routines for uses in typhoon prediction. Our end-to-end procedure combining retrieval, data assimilation, and forecast is similar to the framework developed by Z02, but with a distinctive variation in that we perform a downward instead of upward integration in the retrieval procedure and with the integration starting from a constant 50-hPa field without any prescribed a priori structure. The typhoon circulation from our retrieval is entirely determined objectively from the AMSU observations alone. Even without a prescribed inner core circular vortex structure at the surface as used in the upward integration procedure in Z02, our retrieval procedure produced reasonable patterns of typhoons. The more notable impact of the AMSU data on the assimilated initial condition for prediction is in the modification of the upper-level circulation of the typhoons. With our approach of downward integration, the error accumulates downward such that our AMSU-based estimate of the upper-level circulation may be more accurate than that of the

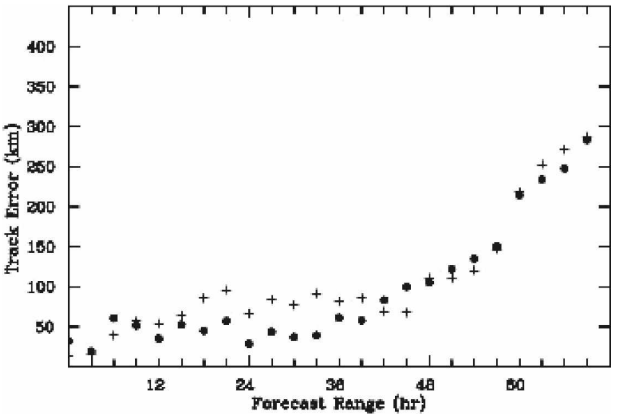

FIG. 16. The absolute forecast error in the typhoon track (km) averaged over the three cases in this study as a function of the forecast lead time from 0 to 72 h. The filled circles and crosses are the forecasts with and without the AMSU input, respectively.

lower-level circulation. Indeed, consistent with these two points, it was demonstrated that the inclusion of the AMSU data helps improve the forecast of typhoon tracks, since the latter depends more on the steering of the typhoons by the upper-level circulation.

At the same time, assimilating only the temperature and velocity fields exclusively derived from the AMSU data in the 3DVAR does not recover the full intensity (minimum SLP) of the typhoons. Other considerations—assimilation with additional sources of observations or imposing of additional (if artificial) corrections on SLP—are needed to improve the forecast of typhoon intensity (e.g., Liang et al. 2007). How this could be done without disrupting the retrieved AMSU-based typhoon structure remains to be investigated.

While the results of this work from the limited cases are encouraging, further studies are needed to compare the pros and cons of the two procedures of upward and downward integration from the statistics of a large number of cases. Previously, Z02 suggested that the use of an upward integration may be beneficial because errors inherent to the AMSU data might be larger at the upper levels. While there may indeed be some errors of this nature at the upper troposphere and lower stratosphere, our results at least showed that they may not be serious enough to upset the whole procedure when a downward integration approach is adopted.

Finally, even within the framework of our procedure, there is still room for improvement just for the retrieval part of the whole procedure. As mentioned in section 2, Bessho et al. (2006) have recently developed a more sophisticated algorithm to correct the effects of scattering in some AMSU channels on the retrieved temperature. These advances in the technique can be incorporated into a future version of our procedure. Another aspect to consider is to combine the AMSU data with other independent observations. One possibility is the Atmospheric Infrared Sounder (AIRS) data that can be used to more accurately estimate the atmospheric state

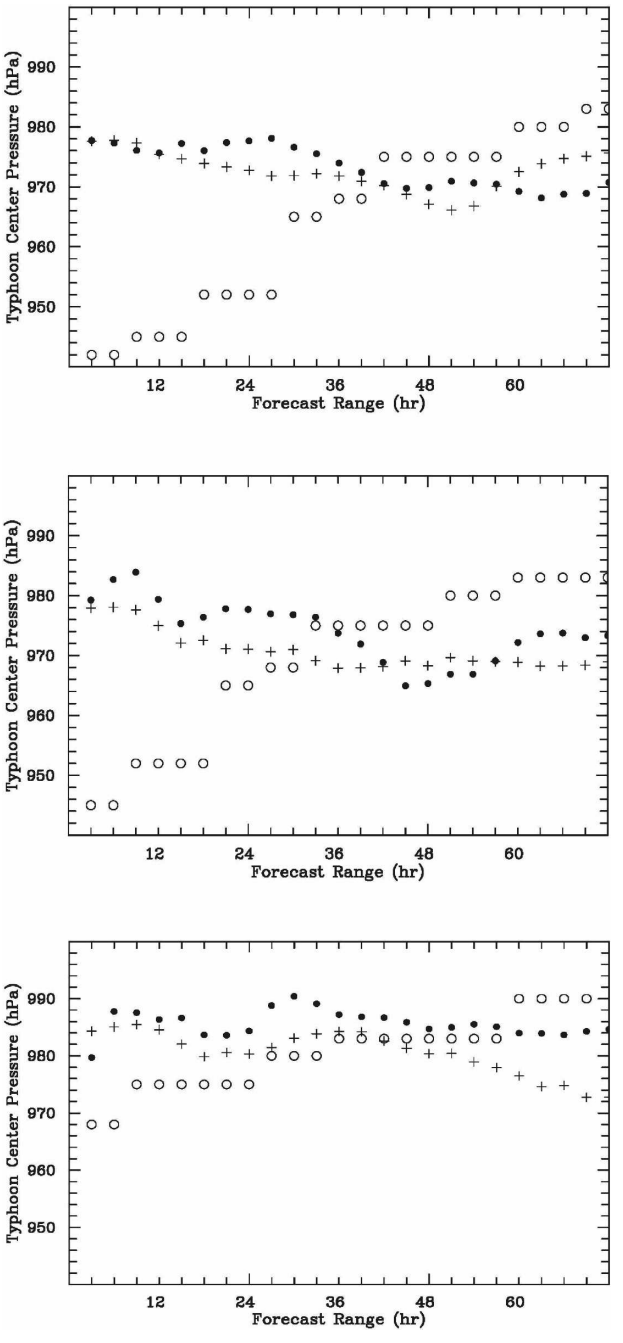

FIG. 17. The observed (open circle, estimates from CWB) and model predicted (cross = control without AMSU input; filled circle = forecast with AMSU input) minimum SLP as a function of time for the three forecast cases with the initial times of (top) 1800 UTC 29 Jun, (middle) 0060 UTC 29 Jun, and (bottom) 1800 UTC 30 Jun, respectively.

at the upper troposphere and lower stratosphere. Note that contamination by clouds would not be a problem for the AIRS observation above the cloud top (e.g., at 50 hPa). One can then have a more accurate upper boundary condition as the starting point for the downward integration. Another possibility is to merge the AMSU data with other relatively high-density in situ observations while they are available. An example is the dropwindsonde observations for selected typhoons in the vicinity of Taiwan from the Dropsonde Observations for Typhoon Surveillance near the Taiwan Region (DOTSTAR) field experiments (Wu et al. 2005). We look forward to future investigations along these directions.

Acknowledgments. The first author thanks Professor Da-Lin Zhang of University of Maryland for his valuable help and instruction and Dr. Tong Zhu and Dr. Fuzhong Weng for helpful discussions. He also thanks Dr. N. Grody for providing valuable help and advice on estimating the precipitation rate used in this study and Dr. Tsan Mo of NOAA NESDIS for providing useful information and advice on the quality of the AMSU data. The authors appreciate useful comments from three anonymous reviewers that helped to improve the quality of this paper.

REFERENCES

Barker, D. M., W. Huang, Y.-R. Guo, A. J. Bourgeois, and Q. N. Xiao, 2004: A three-dimensional variational data assimilation system for MM5: Implementation and initial results. *Mon. Wea. Rev.,* **132,** 897–914.

Bessho, K., M. DeMaria, and J. A. Knaff, 2006: Tropical cyclone wind retrievals from the Advanced Microwave Sounding Unit: Application to surface wind analysis. *J. Appl. Meteor. Climatol.,* **45,** 399–415.

Chen, S.-H., F. Vandenberghe, G. W. Petty, and J. F. Bresch, 2004: Application of SSM/I satellite data to a hurricane simulation. *Quart. J. Roy. Meteor. Soc.,* **130,** 801–825.

Chou, C.-B., C.-Y. Huang, K.-H. Wang, M.-H. Liao, and L.-N. Shee, 2005: The analysis of typhoon parameters by using AMSU data. *Proc. 14th Int. ATOVS Study Conf.,* Beijing, China, Radiation Commission of the International Association of Meteorology and Atmospheric Sciences, 10 pp. [Available online at http://cimss.ssec.wisc.edu/itwg/itsc/itsc14/proceedings.]

Demuth, J. L., M. DeMaria, J. A. Knaff, and T. H. Vonder Haar, 2004: Evaluation of Advanced Microwave Sounding Unit tropical-cyclone intensity and size estimation algorithms. *J. Appl. Meteor.,* **43,** 282–296.

Dudhia, J., 1993: A nonhydrostatic version of the Penn State–NCAR mesoscale model: Validation tests and simulation of an Atlantic cyclone and cold front. *Mon. Wea. Rev.,* **121,** 1493–1513.

Grody, N., F. Weng, and W. C. Shen, 1982: Observation of Hurricane David (1979) using the Microwave Sounding Unit. NOAA Tech. Rep. NESS 88, 52 pp.

——, ——, and R. Ferraro, 2000: Application of AMSU for obtaining hydrological parameters. *Microwave Radiometry and Remote Sensing of the Earth's Surface and Atmosphere,* P. Pampaloni and S. Paloscia, Eds., Brill, 339–351.

Ide, K., P. Courtier, M. Ghil, and A. C. Lorenc, 1997: Unified notation for data assimilation: Operational, sequential, and variational. *J. Meteor. Soc. Japan,* **75,** 181–189.

Jeng, B.-F., H.-J. Chen, S.-C. Lin, T.-M. Leou, M. S. Peng, S. W. Chang, W.-R. Hsu, and C.-P. Chang, 1991: The limited-area forecast systems at the Central Weather Bureau in Taiwan. *Wea. Forecasting,* **6,** 155–180.

Kidder, S. Q., W. M. Gray, and T. H. Vonder Harr, 1978: Estimating tropical central pressure and outer wind from satellite microwave data. *Mon. Wea. Rev.,* **106,** 1458–1464.

——, ——, and ——, 1980: Tropical cyclone outer surface winds derived from satellite microwave sounder data. *Mon. Wea. Rev.,* **108,** 144–152.

——, M. D. Goldberg, R. M. Zehr, M. DeMaria, J. F. W. Purdom, C. S. Velden, N. C. Grody, and S. J. Kusselson, 2000: Satellite analysis of tropical cyclone using the Advanced Microwave Sounding Unit (AMSU). *Bull. Amer. Meteor. Soc.,* **81,** 1241–1259.

Knaff, J. A., S. A. Seseske, M. DeMaria, and J. L. Demuth, 2004: On the influences of vertical wind shear on symmetric tropical cyclone structure derived from AMSU. *Mon. Wea. Rev.,* **132,** 2503–2510.

Liang, X., B. Wang, J. Chan, Y. Duan, D. Wang, Z. Zeng, and M. Leiming, 2007: Tropical cyclone forecasting with model-constrained 3D-Var. II: Improved cyclone track forecasting using AMSU-A, QuikSCAT, and cloud-drift wind data. *Quart. J. Roy. Meteor. Soc.,* **133,** 155–165.

Liou, C.-S., and Coauthors, 1997: The second-generation global forecast system at the Central Weather Bureau in Taiwan. *Wea. Forecasting,* **12,** 653–663.

Rosenkranz, P. W., D. H. Staelin, and N. C. Grody, 1978: Typhoon June (1975) viewed by a scanning microwave spectrometer. *J. Geophys. Res.,* **83,** 1857–1868.

Smith, R. K., 2003: A simple model of the hurricane boundary layer. *Quart. J. Roy. Meteor. Soc.,* **129,** 1007–1027.

Tarbell, T. C., T. T. Warner, and R. A. Anthes, 1981: An example of the initialization of the divergent wind component in a mesoscale numerical weather prediction model. *Mon. Wea. Rev.,* **109,** 77–95.

Velden, C. S., B. M. Goodman, and R. T. Merrill, 1991: Western North Pacific tropical cyclone intensity estimation from NOAA polar-orbiting satellite microwave data. *Mon. Wea. Rev.,* **119,** 159–168.

Wu, C.-C., and Coauthors, 2005: Dropwindsonde observations for typhoon surveillance near the Taiwan region (DOTSTAR): An overview. *Bull. Amer. Meteor. Soc.,* **86,** 787–790.

Zhu, T., D.-L. Zhang, and F. Weng, 2002: Impact of the Advanced Microwave Sounding Unit measurements on hurricane prediction. *Mon. Wea. Rev.,* **130,** 2416–2432.